(Preprint) AAS XX-XXX

HARDWARE DEMONSTRATION AND IMPROVEMENTS OF THE STELLAR POSITIONING SYSTEM

Joel Amert* and Michael Fritzinger†

As the number of Lunar and Martian surface-exploration missions increases, precise surface navigation is becoming critical. Of most interest is navigation techniques that can generate an absolute state without reliance on Earth-based tracking. One such navigation technique is the Stellar Positioning System. Based on the practice of celestial navigation, this approach combines measurements of the body, star field orientation, and time, to calculate an absolute position on the surface of any planetary body with a known gravity field and known orientation in celestial space. A hardware prototype consisting of an inertial measurement unit, star tracker, and accurate time keeping was developed to demonstrate this concept. The stellar positioning system model was refined to fit this hardware, and was demonstrated by conducting live-sky tests in multiple locations around Marshall Space Flight Center in Huntsville, AL. This effort discusses the preliminary testing results, improvements of the stellar positioning system, feasibility for surface exploration missions, and planned further refinements that will improve the performance.

INTRODUCTION

One of the requirements for missions landing on other bodies in the solar system, such as the moon or Mars, is for landing assets to be able to determine their location relative to the body sometime after touchdown. This absolute navigation for both the moon and Mars has usually been done using external tracking systems. Future missions could benefit from autonomously calculating their absolute position on the surface of the moon or Mars in order to reduce dependency on external tracking. One of the options for absolute, autonomous navigation, is called the Stellar Positioning System (SPS), and is an option for future missions to autonomously calculate their position without external input.

STELLAR POSITIONING SYSTEM OVERVIEW

The original Stellar Positioning System is presented in References 1 and 2, which is based on the practice of celestial navigation that has been used successfully on Earth for hundreds of years. This combines measurement of the stars, measurement of the Earth, time, and knowledge of the Earth, to create a position measurement. This was commonly used for navigating the oceans by using a sextant prior to more advanced navigation techniques being developed.

* Aerospace Engineer, ES31 Guidance, Navigation, and Control Hardware Team, NASA/MSFC, Huntsville, Alabama 35811, USA.
† Aerospace Engineer, EV42 Guidance, Navigation and Mission Analysis Branch, NASA/MSFC, Huntsville, Alabama 35811, USA.

A sextant was used by measuring the angular difference between known stars and the horizon, along with the measurement time, to estimate both the latitude and longitude. While this required skilled operators, position readings could be performed within two nautical miles.[3]

The SPS uses similar principles to apply this technique using modern hardware. For this iteration of the SPS, instead of a telescope, a star tracker or camera is used to measure star orientations, and instead of using a measurement of the horizon, either an inclinometer or accelerometers are used to measure the local gravity of the Earth.

HARDWARE OVERVIEW

The current iteration of the SPS uses an Inertial Measurement Unit (IMU) to measure the local gravity, a star tracker to measure the orientation of the star field, and the Pulse-Per-Second (PPS) timing signal from Global Position System (GPS) - a chip scale atomic clock (CSAC) is baselined for use in the flight version to measure the time. This hardware was chosen due to the availability of similar hardware for testing purposes on the ground, as well as availability of proven, high technology readiness level (TRL) components that would simplify the flight version of the system. It is worth noting that many vehicles landing on celestial bodies will already have these components available, making SPS a viable lost-on-surface navigation solution with a limited impact to mass and power.

Inertial Measurement Unit

The selected IMU was the HG9900 from Honeywell.[4] This IMU was chosen due to hardware availability as well as the accelerometers. The HG9900 uses QA2000 accelerometers, while there are IMUs with extensive space heritage that use QA3000 accelerometers, which are identical in form, fit, and function to the QA2000s with improved accuracy and increased environmental testing and reliability.

The flight version of the SPS would use either an IMU with similar accelerometers to the QA3000 or would use two or three separate accelerometers that are hard-mounted to the same rigid plate as the star tracker. The IMU option would simplify the integration and calibration, while the separate accelerometers could potentially increase the accuracy of the system as discussed below.

The HG9900 has the capability to produce accelerometer measurements with a bias of less than 25 micro-g, and a scale factor of less than 100 parts per million.

Star Tracker

The star tracker used was the standard Nano Star Tracker (NST) from Blue Canyon Technologies (BCT).[5] This was selected due to the hardware availability, as well as size and accuracy.

The flight version of the SPS has a star tracker similar to the BCT NST baselined as the star tracker. This simplifies integration of the system due to not needing to run any calibration of the star camera, and only needing to read the output of the star tracker.

The BCT NST has the capability to produce attitude knowledge with approximately 6 arcseconds cross boresight, and 40 arcseconds of attitude error about the boresight.[5]

Time

For hardware testing purposes, the time keeping was done using a GPS receiver and antenna to use GPS time throughout the tests. This was done following analysis showing that the time keeping is not a driving source of error for an SPS system on the Lunar surface, so the hardware testing was limited to determine if the combined system of the star tracker and IMU would be enough to

determine a location estimate, and did not include testing the timekeeping of a clock, which has been tested elsewhere.

The flight version of the SPS has CSAC baselined as the timekeeping. This CSAC time would be referenced to true time prior to launch, or in range of either GPS satellites prior to departure of the Moon, or while in range of Earth-based communications prior to descent to the lunar surface. A CSAC would be accurate to within 0.01 parts per million, resulting in an error on the order of 20 milliseconds after a month of operation. There are CSACs with space heritage which would simplify testing and integration.

Data Recording

For hardware testing, the data recording from the IMU, star tracker, and GPS, was accomplished using two single board computers (SBCs). One of these SBCs was used to record the IMU data, and the other was used to record the star tracker and GPS data. The data was post-processed to time synchronize the data from the two SBCs.

For the flight version, the baseline is using a heritage flight computer that has the capability to read, process, output, and save data from the IMU or accelerometers, the clock, and the star tracker.

Hardware Mounting

One critical component of the SPS is the stability between the orientation of the accelerometers and the orientation of the star tracker. To accomplish this, a two-inch-thick aluminum plate was used, and the IMU and star tracker were securely fastened to the plate as shown in Figure 1 and Figure 2. Neither the IMU nor the star tracker were removed throughout both live sky tests to prevent any inaccuracies with the orientations changing after being removed and re-fastened to the plate.

The flight version of the SPS would either use a star tracker and IMU securely fastened to the same rigid mounting plate, or accelerometers securely fastened to the same plate as the star tracker.

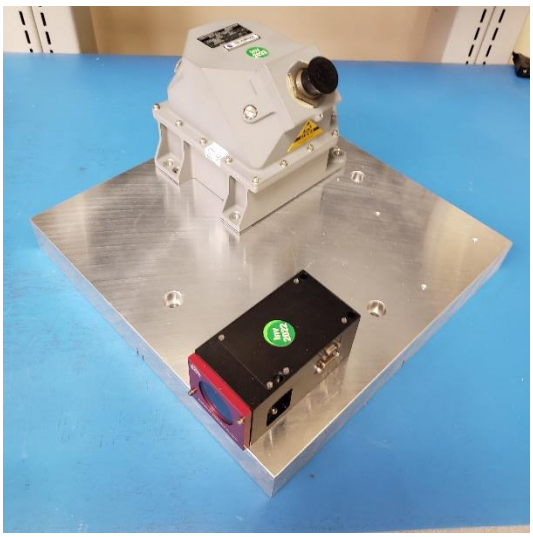

Figure 1. IMU and Star Tracker on the Mounting Plate

Figure 2. SPS Demonstration System Mounted on Tripod

IMPROVEMENTS TO THE STELLAR POSITIONING SYSTEM

In order to calculate the location using SPS, the acceleration in an Earth-fixed coordinate system has to be calculated. This starts with estimating the acceleration due to gravity in the IMU frame. This is then converted to the star tracker frame using the interlock matrix, which is the estimated orientation of the IMU relative to the star tracker. Next, it is converted to inertial coordinates using the star tracker measurement of the star orientation relative to the star tracker. Finally, it is converted to Earth Centered Earth Fixed (ECEF) coordinates by using the time that the star tracker measurement occurred. Combining these into a single equation results in

$$\hat{a}_g^e = \hat{C}_i^e \hat{C}_{st}^i \hat{C}_{IMU}^{st} \hat{a}_g^{IMU} \tag{1}$$

Where $\hat{a}_g^e$ is the acceleration due to gravity as a function of position, $\hat{C}_i^e$ is the conversion from Earth Centered Inertial (ECI, in the J2000 frame) coordinates to Earth Center Earth Fixed Coordinates (ECEF) frame, $\hat{C}_{IMU}^{st}$ is the conversion from the IMU sensor frame to the star tracker frame, and $\hat{a}_g^{IMU}$ is the measured acceleration out of the IMU in the IMU sensor frame. Once the acceleration is known in the ECEF reference frame, it can be converted to position using well-known gravity models as shown below.

Interlock Matrix Calculation

In order for the SPS to accurately calculate the position, the orientation between the star tracker and the accelerometers has to be known more accurately than the as-built configuration would end up using only the drawing specifications. In a flight configuration, the interlock matrix would be calculated prior to integration in the vehicle. For this hardware demonstration, this interlock matrix was calculated using the first iteration of the outdoor testing at a known position, assuming that the location is known.

Two methods to calculate this interlock matrix were identified. For both methods, Equation (1) was rearranged to form the equation

$$\left(\hat{C}_i^e \hat{C}_{st}^i\right)^{-1} \hat{a}_g^e = \hat{C}_{IMU}^{st} \hat{a}_g^{IMU} \tag{2}$$

The left side of Equation (2) was then combined to form the acceleration measured in the star tracker frame, resulting in the equation

$$\hat{a}_g^{st} = \hat{C}_{IMU}^{st} \hat{a}_g^{IMU} \tag{3}$$

Once this equation is written as shown in Equation (3), this becomes the classic and well-known problem of measuring vectors in two different coordinate systems and calculating the orientation between the different coordinate systems. One method to calculate this orientation between the coordinate systems is to rotate calculate average measurements at two different orientations. This results in four total measurements: $\hat{a}_g^{st}{}_1$, $\hat{a}_g^{IMU}{}_1$, $\hat{a}_g^{st}{}_2$, and $\hat{a}_g^{IMU}{}_2$. These are then used to calculate $\hat{C}_{IMU}^{st}$ using the equation

$$\hat{C}_{IMU\,coarse}^{st} = \left[\hat{a}_g^{st}{}_1 \quad \hat{a}_g^{st}{}_2 \quad \hat{a}_g^{st}{}_1 \times \hat{a}_g^{st}{}_2\right]\left[\hat{a}_g^{IMU}{}_1 \quad \hat{a}_g^{IMU}{}_2 \quad \hat{a}_g^{IMU}{}_1 \times \hat{a}_g^{IMU}{}_2\right]^{-1} \tag{4}$$

The downside to this approach is that only averaged data over two orientations can be used for the calculation while keeping the equation simple, while more would be beneficial. Instead of using Equation (4), a Kalman filter could be used; however, since this estimate is only needed post-processing, and the gyroscopes were not used during these tests, using a least squares estimate to post-process the data to refine the alignment has the same accuracy as a Kalman filter. The cost function for the least squares estimation is calculated using the equation

$$J = \left|\left(\hat{C}_i^e \hat{C}_{st}^i\right)^{-1} \hat{a}_g^e - \hat{C}_{IMU}^{st} \hat{a}_g^{IMU}\right| \tag{5}$$

With this cost function calculated for each star tracker measurement, a least squares estimate can be used to calculate a refined interlock matrix.

Geopotential Model

In order to calculate the position accurately, accurate knowledge of the gravity vector is required as a function of location. In the original SPS, a lookup table was used for the gravity model. This has the advantage of being faster to run – an interpretation between the look up table values is all that is required; however, this has the disadvantage of being limited by the size of the lookup table as to what locations in which the SPS will work.

To eliminate the location limitation, instead of a lookup table, a full spherical harmonic geopotential was used. This also increases the options for what geopotential models can be used – gravity models are generally released using spherical harmonic coefficients, so the coefficients can change based on the body that the system is on or easily updated as additional models become available. This has the drawback of being slower to run; however, there are well-known methods to increase the run time in order to get the system to be able to run in real time.[6]

Any implementation of the spherical harmonic coefficients would work, and for this testing a forward column recursion, calculating both the gravity and the gravity Jacobian, was used as shown in Reference 6. This has the advantage of being efficient to implement and allows for future optimization of the system if a first or second order expansion of the gravity model is needed to increase run time. On the Earth, the centripetal acceleration caused by the Earth's rotation is removed from the geopotential prior to being used in the equations, but this would not have to occur on the Lunar surface due to the lower rotation rate of the Moon.

Initial Location

The original SPS equations from References 1 and 2 require an estimation of the initial location. While for most applications, an estimate of the initial location would be known, for other applications it would be beneficial to have the capability to calculate the location without any prior knowledge.

Ideally, once the gravity estimate in ECEF coordinates is calculated, the inverse function of the gravity model would be used to calculate the position. However, an inverse function for a spherical harmonic geopotential does not exist, so this calculation is not possible with a full fidelity gravity model. For this reason, an estimation of the gravity model can be used to calculate the initial position in order to initialize the higher order model. Using a perfect sphere estimate for the gravity, Equation (1) becomes

$$\frac{-\hat{r}_{coarse_1}\mu}{a^3} = \hat{C}_i^e \hat{C}_{st}^i \hat{C}_{IMU}^{st} \hat{a}_g^{IMU} \tag{6}$$

Where a is the Earth radius and μ is the gravitational parameter. Solving for position results in the equation

$$\hat{r}_{coarse_1} = -\frac{a^3}{\mu} \hat{C}_i^e \hat{C}_{st}^i \hat{C}_{IMU}^{st} \hat{a}_g^{IMU} \tag{7}$$

Once this is calculated, this can be further refined by accounting for the centripetal acceleration using the equation

$$\hat{r}_{coarse_2} = -\frac{a^3}{\mu} (\hat{C}_i^e \hat{C}_{st}^i \hat{C}_{IMU}^{st} \hat{a}_g^{IMU} + \Omega \times \Omega \times \hat{r}_{coarse_1}) \tag{8}$$

Where Ω is the rotation rate vector of the body. Equation (8) can be repeated as desired to provide an updated coarse location estimate, but this was found not to be necessary in order to produce an initialization for the higher fidelity calculations.

Position Calculation

Once the coarse estimate is known, this can be further refined using a Taylor series expansion of Equation (1) through the equations

$$\delta g_i = g(\hat{r}_i) - (\hat{C}_i^e \hat{C}_{st}^i \hat{C}_{IMU}^{st} \hat{a}_g^{IMU} + \Omega \times \Omega \times \hat{r}_i) \tag{9}$$

$$\hat{r}_{diff_i} = G_{r_i}^{-1} \delta g_i \tag{10}$$

$$\hat{r}_{i+1} = \hat{r}_i + \hat{r}_{diff_i} \tag{11}$$

Where $g(\hat{r}_i)$ is the geopotential model using the previously calculated location as an input, $G_{\hat{r}_i}$ is the gravity Jacobian matrix calculated at $\hat{r}_i$, and $\hat{r}_{i+1}$ is the updated location estimate. This loop can be run until the updated position is within pre-set bounds of the previous location.

HARDWARE TESTING RESULTS

To test the SPS using the hardware setup, two outdoor, live sky tests were run, about two weeks apart, and in locations separated by approximately 2.75km. The test setup used during these tests is shown in Figure 3. For each test, data was recorded at the maximum rate available from both the IMU and the star tracker – 300Hz from the IMU and 5 Hz from the star tracker. The star tracker data was time stamped with the GPS time as it was recorded, and the IMU data was post-processed to align the data to the star tracker data. Since the IMU data is output at a higher rate than the star

tracker data, it was averaged to produce a measurement at the same rate as the star tracker measurement.

Data was collected for approximately one hour at each location, in four different orientations of approximately fifteen minutes each. A tripod with a manual adjustable tilt and azimuth assembly was used as shown in Figure 3, and the system was allowed to settle after movement to reduce vibrations effects on the measurements.

Figure 3. SPS Demonstration System During a Live Sky Test

Interlock Matrix Calculation Results

In order for SPS to accurately calculate the location, the orientation of the star tracker relative to the IMU sensor frame has to stay at a known and fixed orientation. To test this, the interlock matrix was calculated using data from both outdoor live sky testing runs. This data is shown in Table 1.

Table 1. Table of Orientation of the IMU relative to the Star Tracker for both tests

	Yaw (degrees)	Pitch (degrees)	Roll (degrees)
Run 1	-179.857	-0.006	-80.135
Run 2	-179.850	-0.020	-80.145

As shown in Table 1, the change in orientation of the IMU relative to the star tracker was constant within 0.02 degrees. This would correspond to an error of approximately 2km on the surface of the Earth. This shows that the IMU sensor frame does potentially shift a measurable amount during testing and that this error will have to be eliminated to increase the overall performance of the system.

Position Calculation Results

In order to test that the SPS in this hardware configuration can accurately determine the location, first the interlock matrix was calculated from the run 1 data, then the location was calculated using the location two data. The position was calculated for each star tracker measurement and averaged over the hour-long data collection for both east/west error and north/south error. This is shown in Table 3.

Table 2 Average Position Error

East/West Position Error	North/South Position Error	Total Horizontal Position Error
-296m	-298m	421m

As Table 2 shows, the position error from averaging the measurements over an hour results in an error of 421 meters. In addition to identifying average error, the independent position calculations for each star tracker measurement were also identified and plotted. This is shown in Figure 4.

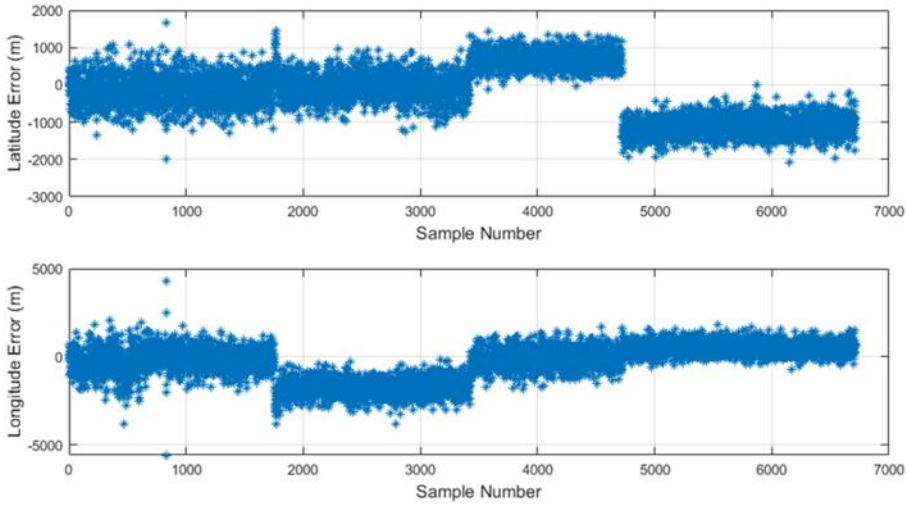

Figure 4. Position Data for Each Star Tracker Measurement

As Figure 4 shows, while the average error converges to 421m, the error from each orientation of the system changes to a different error in each orientation, and the final position error appears to be random. The average error for each orientation is shown in Table 3.

Table 3. Position Error, Averaged at Each System Orientation

Position Number	East/West Position Error (m)	North/South Position Error (m)	Total Horizontal Position Error (m)
1	-144	-194	242
2	-51	-1706	1707
3	689	-141	703
4	-1114	504	1223

This figure shows that while the average position error converges to 421m, the error from each orientation can be more than 1700 m, and that the error changes for each rotation of the system. This indicates that there are potentially additional error sources that have not been accounted for in the equations.

POTENTIAL UNACCOUNTED ERROR SOURCES

Since Figure 4 and Table 3 show that there is potentially unaccounted for errors in the equations, a few different potential sources of this error were analyzed to determine if it is what caused the change in error.

Atmospheric Refraction

Since the star tracker is meant to be used in space, it does not account for any atmospheric effects on star light. It is well known that as light passes through the atmosphere, refraction will cause the light to appear to change orientation when viewed from the ground, for a few models of this effect, see Reference 7. This was corrected for by using Bennet's equation as shown in Reference 7 and the results are shown in Table 4.

Table 4. Overall Average Position Error while Accounting for Atmospheric Refraction

East/West Position Error	North/South Position Error	Total Horizontal Position Error
-659m	-163m	679m

When applied to the test data, for both the interlock matrix and the second data, this resulted in a location error of 679m as shown in Table 4, compared to 421m without this effect modeled. This shows that this was not the main driving error source in the data.

Velocity Aberration

Velocity aberration is caused by the velocity of the observation cameras relative to the motionless stars. The main velocity is caused by the rotation of the Earth around the sun, and this velocity can cause variation in the observed orientation of the stars by up to 20.5 arcseconds.[8] While the star tracker has the capability to automatically correct for the velocity aberration, this feature was not turned on during the tests, and instead was accounted for during post-processing of the data. This was corrected by using the equation from Reference 8 and the results are shown in Table 5.

Table 5. Overall Average Position Error while Accounting for Velocity Aberration

East/West Position Error	North/South Position Error	Total Horizontal Position Error
237	291	376

When applied to the test data, for both the interlock matrix and the second data, this resulted in a location error of 376m, compared to 421m without this model, showing that this was not the main driving error source in the data.

Combining both velocity aberration and atmospheric refraction results in Table 6, which shows that there is still an unidentified error source that has not been corrected for.

Table 6. Overall Average Position Error while Accounting for both Atmospheric Refraction and Velocity Aberration

East/West Position Error	North/South Position Error	Total Horizontal Position Error
-125	426	444

Uncompensated IMU Errors

Another potential source of error is uncompensated errors in the accelerometers. One such error is the accelerometers shifting relative to the IMU mounting feet. The IMU sensors are not rigidly mounted to the frame – they are mounted on isolators meant to dampen vibrations, and therefore have the potential to shift, would could cause some of the errors in the data.

Another potential error source is the residual bias and scale factor errors in the accelerometers. If a single accelerometer was directly measuring the gravity vector, with the gravity vector not being split between any of the other accelerometers, the tilt error caused by the accelerometer errors would be solely a function of the accelerometer bias, with the tilt error approximately equaling the bias – a 25 µg bias would cause a tilt error of approximately 25 µradians. However, for the SPS testing, the IMU was oriented in an orientation that meant that multiple of the accelerometers were measuring the gravity vector, so the scale factor would also impact the tilt error. A 100 PPM scale factor error combined with the 25µg bias would cause a 75 µradians tilt error in the worst-case orientation, and this tilt error would change based on the IMU's orientation relative to the gravity vector.

Without an accurate, real-time calibration of the IMU errors, the scale factor errors and potential shifts of the ISA block are unobservable from each other, and appear as a single tilt error relative to the mount frame. To test this combination of errors, the IMU was mounted to a three-axis rate table, calculating the orientation of the sensor block relative to the rate table, and calculating the error in the pitch and roll axes for multiple different table orientations. This showed an error of more than 0.01°, or 36 arcseconds, which would cause a position error of more than 1km, showing that it appears to be the driving source of uncompensated error in the system. Without an accurate estimation of the IMU error sources, it is random and not able to be removed from the data.

In order to compensate for the scale factor errors, Equation (1) could be re-written to include the scale factor errors. Including these errors, Equation (1) becomes

$$\hat{a}_g^e = \hat{C}_i^e \hat{C}_{st}^i \hat{C}_{IMU}^{st} \left(\hat{a}_g^{IMU\prime} \begin{bmatrix} 1+x_{SF} & 0 & 0 \\ 0 & 1+y_{SF} & 0 \\ 0 & 0 & 1+z_{SF} \end{bmatrix} \right)' \tag{12}$$

These scale factor errors can be included in the least squares estimation from Equation (5) to which the cost function becomes

$$J = \left| \left(\hat{C}_i^e \hat{C}_{st}^i \right)^{-1} \hat{a}_g^e - \hat{C}_{IMU}^{st} \left(\hat{a}_g^{IMU\prime} \begin{bmatrix} 1+x_{SF} & 0 & 0 \\ 0 & 1+y_{SF} & 0 \\ 0 & 0 & 1+z_{SF} \end{bmatrix} \right)' \right| \tag{13}$$

Estimating these scale factor errors results in the performances shown in Table 7, and accounting for all above errors results in the performances shown in Table 8 and Table 9.

Table 7 Average Position Error while Estimating Accelerometer Scale Factors

East/West Position Error	North/South Position Error	Total Horizontal Position Error
-272	-209	343

Table 8 Average Position Error while Accounting for all Mentioned Error Sources

East/West Position Error	North/South Position Error	Total Horizontal Position Error
74	446	452

Table 9 Position Error at Each System Orientation while accounting for all mentioned error sources

Position Number	East/West Position Error (m)	North/South Position Error (m)	Total Horizontal Position Error (m)
1	190	627	655
2	138	323	351
3	832	1389	1619
4	-624	73	628

As shown in Table 8 and Table 9, estimating these scale factor errors does not eliminate the error. With only estimating the scale factor the performance becomes slightly better, however with accounting for all the above-mentioned errors the performance becomes slightly worse. This could be due to the sensor assembly block in the IMU shifting during each orientation, or the scale factors changing between run 1 and run 2.

This error source can be eliminated in future designs of the system by using high-quality and hard-mounted accelerometers instead of a vibrationally isolated assembly. While not as robust to shock or vibration, hard-mounted accelerometers would reduce the change of the IMU sensor assembly relative to the star tracker reference frame.

FUTURE WORK AND CHALLENGES

Some of the initial future work involve building and testing a system using higher quality, independent accelerometers instead of a pre-built IMU. While this does involve additional complexity in both the hardware design and software processing, this has the potential to increase the overall accuracy of the system. The challenge of this approach is that this would use newer accelerometers without space heritage.

Another option is to use independent accelerometers of the same design as used during these tests. This would have the benefit of being hard-mounted, which would eliminate any error caused by the ISA block shift, but the scale factor error would still be included. Accuracy of this type of system could be increased by developing specific orientations to run the system. This could allow the calculation of scale factor estimates during the second run without assuming that the position is known. This could increase the accuracy of the system while maintaining the flight heritage of the accelerometers; however, would increase the complexity of the system by requiring it to change orientations while in use.

One of the largest challenges with building a flight version of the SPS is demonstrating that it is necessary and worth spending the time, effort, and funding to design, build, test, then operate the hardware. The SPS would have a very limited use case. It would only be beneficial in the instances where there is sufficient knowledge of the geopotential field of the body, there are no methods of external tracking or there are more assets on the surface of the body than can be easily remotely tracked, and there is no other system in place for surface tracking. The SPS can be replaced by

systems similar to GPS – if a similar system was built for the lunar surface, it would eliminate the need of a system using SPS equations. The SPS can also be replaced by having a good solution for the touchdown coordinates of landers and using on-board rover navigation to integrate the position.

CONCLUSION

The Stellar Positioning System is a method for absolute navigation on the surface of any planet or moon with a known geopotential field. It was successfully demonstrated on the surface of the Earth using hardware that has similar components with high space heritage. The equations for SPS were updated to fit the hardware. The overall error was on the order of 450 m, which would correspond to 125 m on the surface of the lunar surface. The driving source of this error appeared to be the quality of the accelerometers; with this performance is expected to increase with using higher quality accelerometers. While the long-term use case for a SPS system is potentially limited, this shows that there is potential to use the SPS on the surface of the moon without significant hardware development or navigation infrastructure. A few potential options were identified to increase the performance of the system.

ACKNOWLEDGMENTS

The authors would like to thank the interns who worked on this project. Anthony Gardner developed the initial simulation while working as an intern over the summer of 2020 and set up the initial equations for use with an IMU. Savannah Flaherty worked as an intern during Fall 2021 and set up the hardware used for the outdoor testing, including designing the mounting plate, developing the hardware needed for reading the star tracker with GPS time tags, assisting with running both live sky tests, and running the initial processing of the hardware data through the initial SPS algorithms.

REFERENCES

1 J.J. Parish, A.S. Parish, M.S. Swanzy, D. Woodbury, D. Mortari, and J.L. Junkins, "Stellar Positioning System (Part I): Applying Ancient Theory to a Modern World", AIAA/AAS Astrodynamics Specialist Conference, 2008.

2 D. Woodbury, J.J. Parish, A.S. Parish, M.S. Swanzy, R. Denton, D. Mortari, and J.L. Junkins, "Stellar Positioning System (Part II): Overcoming Error During Implementation", AIAA/AAS Astrodynamics Specialist Conference, 2008.

3 R. Malkin, "Understanding the Accuracy of Astro Navigation", Journal of Navigation, 2014.

4 Honeywell Aerospace, "HG9900 Inertial Measurement Unit", 2018.

5 Blue Canyon Technologies, "Star Trackers", 2022.

6 J. Amert, E. Anzalone, T.E. Oliver, "Efficient On-Orbit Singularity-Free Geopotential Estimation", AAS GN&C Conference, 2018.

7 T. Wilson, "Evaluating the Effectiveness of Current Atmospheric Refraction Models in Predicting Sunrise and Sunset Times", Open Access Dissertation, Michigan Technological University, 2018.

8 C.E. Mungan, "A Pictorial Explanation of Stellar Aberration", The Physics Teacher Vol. 57, 2019.